

Conformational Stability and Binding Properties of Porcine Odorant Binding Protein

Tatiana V. Burova,^{‡,§} Yvan Choiset,[§] Christophe K. Jankowski,^{||} and Thomas Haertlé*,[§]

Institute of Biochemical Physics of the Russian Academy of Sciences, Vavilov Strasse 28, 117813 Moscow, Russia, Faculté des Etudes Supérieures et de la Recherche, Université de Moncton, Moncton, New Brunswick, Canada E1A3E9, and Laboratoire d'Etude des Interactions des Molécules Alimentaires, Institut National de la Recherche Agronomique, BP 71627, 44316 Nantes Cedex 03, France

Received April 2, 1999; Revised Manuscript Received August 5, 1999

ABSTRACT: Apparently homogeneous odorant binding protein purified from pig nasal mucosa (pOBP) exhibited subunit molecular masses of 17 223, 17 447, and 17 689 (major component) Da as estimated by ESI/MS. According to gel filtration, this protein, its truncated forms, and/or its variants are homodimeric under physiologic conditions (pH 6–7, 0.1 M NaCl). The dimer \rightleftharpoons monomer equilibrium shifts toward a prevalent monomeric form at pH <4.5. Velocity sedimentation reveals a monomeric state of OBP at both pH 7.2 and 3.5, indicating a pressure-induced dissociation of the homodimer. High-sensitivity differential scanning calorimetry (HS-DSC) shows that the unfolding transition of pOBP is reversible at neutral pH. It is characterized by the transition temperature of 69.23 °C and an enthalpy of 391.1 kJ/mol per monomer. The transition heat capacity curve of pOBP is well-approximated by the two-state model on the level of subunit, indicating that the two monomers behave independently. Isothermal titration calorimetry (ITC) shows that at physiological pH pOBP binds 2-isobutyl-3-methoxypyrazine (IBMP) and 3,7-dimethyloctan-1-ol (DMO) with association constants of 3.19×10^6 and $4.94 \times 10^6 \text{ M}^{-1}$ and enthalpies of –97.2 and –87.8 kJ/mol, respectively. The binding stoichiometry of both ligands is nearly one molecule of ligand per homodimer of pOBP. The interaction of pOBP with both ligands is enthalpically driven with an unfavorable change of entropy. The binding affinity of pOBP with IBMP does not change significantly at acidic pH, while the binding stoichiometry is nearly halved. According to HS-DSC data, the interaction with IBMP and DMO leads to a substantial stabilization of the pOBP folded structure, which is manifested by the increase in the unfolding temperature and enthalpy. The calorimetric data allow us to conclude that the mechanism of binding of the studied odorants to pOBP is not dominated by a hydrophobic effect related to any change in the hydration state of protein and ligand groups but, most likely, is driven by polar and van der Waals interactions.

Odorant binding proteins (OBPs) are known to be members of the lipocalin superfamily (1). This superfamily includes several small secretory proteins often interacting specifically with small mostly hydrophobic ligands. OBPs were identified in bovine olfactory mucosa (2–4), in mucosa of rats (5), mice (6), rabbits, and pigs (7), and in other species (8). The identification of OBPs was initially based on their ability to bind 2-isobutyl-3-methoxypyrazine (IBMP),¹ a low-threshold odorant which is usually described as “bell pepper smell” (4). Later, a large variety of odorants of different classes were shown to bind with high affinity to OBPs (9). Interactions of OBPs free or with bound ligands with olfactory receptors remain to be confirmed.

The physiological function of OBPs is not well understood. Two hypotheses prevail: (i) OBPs play a role in odorant concentration and transport to and from receptors (5, 9), and (ii) they act as low-specificity clearance agents trapping and removing potentially noxious substances (1), thus maintaining the receptor binding sites in a state of readiness.

Relatively intense studies aimed at the elucidation of binding properties and mechanisms were carried out for bovine OBP with a series of ligands, such as 2-isobutyl-3-methoxypyrazine (IBMP) and 3,7-dimethyloctan-1-ol (DMO) (9). It was demonstrated that the binding of these odorants is negatively cooperative and exhibits a stoichiometry of one ligand molecule per one molecule of OBP homodimer (10). It is still unclear, however, whether the ligand binds to only one of two monomers in the dimer or if a single binding site is formed by two monomers. In other words, it is not clear which form of bovine OBP is functionally active: monomeric, dimeric, or both. The three-dimensional structure of the dimeric form of bovine OBP revealed dimerization by so-called “domain swapping” which could form a putative binding site on the dimer interface (11). Another interpretation of crystallographic data suggested the existence of identical internal binding sites on each monomer (12). In such a case, negative cooperativity could be promoted by the tight interlocking of the monomers (13).

* To whom correspondence should be addressed. Telephone: (011 332) 40 67 50 91. Fax: (011 332) 40 67 50 84. E-mail: tom@haertle.nantes.inra.fr.

[‡] Institute of Biochemical Physics of the Russian Academy of Sciences.

[§] Institut National de la Recherche Agronomique.

^{||} Université de Moncton.

¹ Abbreviations: POBP, porcine odorant binding protein; BLG, bovine β -lactoglobulin; ESI/MS, electrospray ionization mass spectrometry; HS-DSC, high-sensitivity differential scanning calorimetry; ITC, isothermal titration calorimetry; IBMP, 2-isobutyl-3-methoxypyrazine; DMO, 3,7-dimethyloctan-1-ol; IEF, isoelectric focusing; LDPC, lysophosphatidylcholine (C_{16}).

Porcine OBP (pOBP) was reported to be monomeric in solution (7, 14). No domain swapping was ever detected in pOBP (14). Crystallographic studies suggested that a putative binding site for the odor molecule is located inside the β -barrel of pOBP. However, this remains unconfirmed experimentally.

OBP binding studies were carried out with an equilibrium binding assay with radioactively labeled ligands (9). This approach does not provide information about the physical nature of protein–ligand interactions. Nor it is clear what the driving force for ligand binding by OBP might be. Is this process entropically driven as was suggested for other lipocalins (15) and as is believed to be characteristic of hydrophobic binding? Does ligand accommodation require a prior or concomitant conformational change of OBP? The answers to these questions are crucial for understanding the role these proteins may play in olfaction.

In this paper, the results of the thermodynamic study of conformational stability and binding properties of porcine OBP by high-sensitivity differential scanning calorimetry (HS-DSC) and isothermal titration calorimetry (ITC) are reported and discussed.

MATERIALS AND METHODS

Protein Purification. OBP was isolated using the protocol of Dal Monte et al. (7) with slight modifications. Porcine olfactory mucosa was collected from pig heads stored at 4 °C for 24 h after slaughter. The collected tissue was homogenized mechanically and washed with 50 mM Tris-HCl buffer (pH 8.0) in the presence of protease inhibitor cocktail (Boehringer). After filtration, the filtrate was acidified to pH 4.5 with HCl, left overnight at 4 °C, and then centrifuged at 4000g for 15 min at 4 °C. The supernatant was adjusted to pH 8.0 and chromatographed on the XK 50 mm \times 300 mm Streamline DEAE column (Pharmacia). Its elution was performed using a linear gradient from 0.15 to 0.5 M NaCl in 50 mM Tris-HCl buffer (pH 8.0). Fractions that eluted at 0.25–0.35 M NaCl were pooled, rechromatographed on the XK 26 mm \times 200 mm Q Sepharose HP column (Pharmacia) using the same buffer, and analyzed by SDS–PAGE. Fractions exhibiting a major band at 22.0 kDa were pooled and applied on the XK 26 mm \times 600 mm Superdex 75 preparative grade gel filtration column (Pharmacia) eluted at the rate of 4 mL/min with 50 mM phosphate buffer, containing 0.15 M NaCl (pH 7.2).

The protein obtained after gel filtration migrated as a single 22.0 kDa band on a 13% SDS–PAGE gel and exhibited a single peak on reverse-phase HPLC. To eliminate possible endogenous ligands, the protein preparation was subjected to the extraction procedure according to the method of Folch et al. (16). The final protein preparation was lyophilized and stored at –20 °C.

2-Isobutyl-3-methoxypyrazine (IBMP) and 3,7-dimethyloctan-1-ol (DMO) were purchased from Aldrich. All reagents were analytical grade.

Isoelectric Focusing. The isoelectric point of the purified pOBP was estimated by isoelectric focusing using precast Servalyt Precotes Gels (pH 3–6).

Mass Spectrometry. The ESI (electrospray ionization) mass spectra were recorded on a Nermag-1010 (Quad Service) single-quadrupole mass spectrometer. The ESI source of

Analytica was used within a mass to charge (m/z) ratio range of 80–2000. The Spectral-30, version 3.7, data system, coupled to the Nermag instrument, was used for calculation (MS Chem Station Software). The peptide sample in demineralized water, in up to 50:50 water/methanol (Merck), or in acetonitrile (C. Erba, 99.8% HPLC grade) was introduced into the ESI source at a rate of 2–3 μ L/min with the syringe pump (Harvard Apparatus, Cambridge, MA). The ESI was performed in the positive ion mode; the ES needle tension was kept at 3.5 kV. The N₂ stream (10 L/min) heated at 150 °C was circulated as a counter-current gas. The lens and quadrupole voltages were optimized to obtain a maximal ion current for electrospray ionization. The calibration of the apparatus was carried out using standard β -lactoglobulin solution with the detection limits set on the presence of four peptides in the mixture as reported by Smith et al. (17).

Some of the analyses were also performed on a Quattro II (Micromass) apparatus under similar conditions (sample injection at a rate of 10 μ L/min, source temperature of 80 °C). Molecular mass determination was achieved using several (usually five to seven) polyprotonated pseudomolecular ion masses.

Gel Filtration. A XK 16 mm \times 600 mm Superdex 75 column (Pharmacia) was used for analytical gel filtration chromatography. The elution was carried out at a rate 0.4–0.8 mL/min with 50 mM potassium phosphate and 0.1 M NaCl or with 50 mM glycine and 0.1 M NaCl. The column was calibrated with LMW Gel Filtration Kit Pharmacia standards covering a molecular mass range of 12.5–67.0 kDa.

Reverse-Phase HPLC. Analytical reverse-phase HPLC was carried out with the Nucleosil 300-5 C8 4 mm \times 70 mm column (Interchim) using a linear 25 min gradient from 0.11% aqueous TFA to the acetonitrile/water mixture (60:40), with 0.09% TFA.

Velocity Sedimentation. Velocity sedimentation was carried out using the MOM 3170B ultracentrifuge (Hungary) at 50 000 rpm and 25 °C. The protein concentration in buffer was 3–5 mg/mL.

Circular Dichroism Spectroscopy. Circular dichroism spectra were recorded using the Jobin Yvon CD6 dichrograph. The spectra were an average of 10 accumulated scans with subtraction of the baseline recorded for buffer solution [10 mM potassium phosphate and 1 mM EDTA (pH 6.6) or 10 mM sodium borate (pH 3.5)]. The protein concentration was 0.6–1.1 mg/mL. The cylindrical cells that were used had a path length of 0.01 cm in the case of far-UV spectra (180–260 nm) and 0.5 cm for the 250–320 nm spectral region. Deconvolution of the far-UV spectra was carried out using the Provencher-Glökner algorithm (18).

Isothermal Titration Microcalorimetry (ITC). Titration experiments were carried out at 36 °C with the isothermal titration microcalorimeter MCS System (MicroCal). Protein solutions were prepared by dialysis against a corresponding buffer at 4 °C for 24 h. Ligand stock solutions were prepared in ethanol, and the concentration was determined by weight. Ligand solutions for titration were prepared by dilution of stock solutions with buffer taken after protein dialysis. The protein concentration in the 1.36 mL calorimetric cell was of 0.04–0.08 mM for pOBP subunits. The ligand concentration in the syringe was between 0.2 and 0.5 mM. The ethanol content in the ligand solution in buffer did not exceed 1%.

Injections (10 μ L) of ligand solution into pOBP solution were carried out at time intervals of 240 s. Ligand–protein titration curves were corrected for the heat of ethanol dilution by subtraction of the blank titration curves obtained by titration of buffer in the cell with the same ligand solution in the syringe. Analysis of calorimetric data was carried out with Origin 4.1 (MicroCal). Binding parameters such as the number of binding sites (n), the binding constant (K_b , M^{-1}), and the binding enthalpy (ΔH_b , kJ/mol of bound ligand) were determined as parameters of fitting of experimental binding isotherms.

High-Sensitivity Differential Scanning Microcalorimetry (HS-DSC). DSC measurements were carried out with the high-sensitivity differential scanning microcalorimeter VP-DSC (MicroCal) within the temperature range of 6–110 $^{\circ}$ C, at a heating rate of 1 K/min and excess pressure of 32 psi. The volume of the calorimetric cell was 0.5 mL, and the protein concentrations that were used were 0.1–0.5 mg/mL. Protein solutions for DSC measurements were prepared by dialysis against a corresponding buffer at 4 $^{\circ}$ C overnight. The protein concentration in solution after dialysis was determined spectrophotometrically assuming an E_{278} of 12.2 $mM^{-1} cm^{-1}$. This value of the extinction coefficient for pOBP was calculated from its amino acid composition according to the method of Pace et al. (19). The amino acid composition of pOBP was taken from the Swiss-Prot database (P81245). Primary data processing was carried out using Origin 4.1 (MicroCal). Molar heat capacity curves of the protein were fitted with SigmaPlot 3.2.

RESULTS

Characterization of the Purified Protein. The purification protocol used in this work was similar to that published previously for pig OBP (7) with an additional stage of extraction with organic solvent for eliminating potential endogenous ligands. The purified protein preparation was essentially homogeneous as judged by gel electrophoresis (SDS–PAGE), reverse-phase HPLC, and isoelectric focusing (IEF). The apparent molecular weight of pOBP in denaturing conditions measured in 13% SDS–PAGE was estimated to be 22 kDa. Mass spectrometry indicated, however, a molecular mass of 17.7 kDa, which is in agreement with the molecular mass calculated from the pOBP sequence. Similar molecular masses of pOBP were also found recently by Paolini and co-workers (20). According to isoelectric focusing, the isoelectric point of pOBP is about 4.1 which is close to the value reported previously (7).

During gel filtration at pH 7.2, purified pOBP eluted at an apparent molecular mass of 34 kDa (Figure 1A), indicating that at physiological pH this protein is in a dimeric form. At pH 3.2, pOBP eluted at an apparent molecular mass of 16.5 kDa (Figure 1B), corresponding to the monomeric form of this protein. Gel filtration data were obtained within the pH range of 7.2–3.0 for pOBP and bovine β -lactoglobulin B (BLG) in parallel. The latter was chosen as a standard with the well-characterized pH-dependent dimerization equilibrium to double check the gel filtration used for the characterization of pOBP and lipocalins in general. A single elution peak was observed for both pOBP and BLG within the whole pH range that was studied. The apparent molecular mass calculated for both proteins from the position of the peak maximum reveals a pH-dependent transition corre-

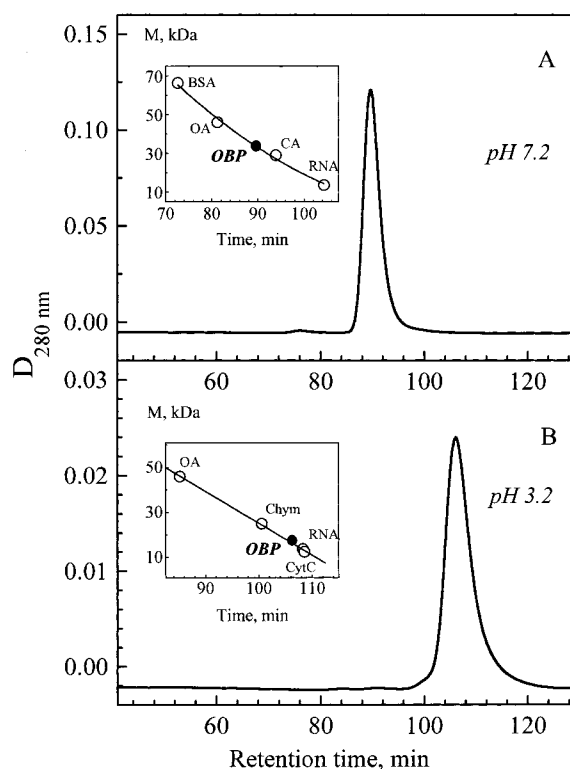


FIGURE 1: Gel filtration elution profiles of pOBP at pH 7.2 (A) and 3.2 (B). Insets show the corresponding calibration curves obtained using the following globular protein standards: bovine serum albumin (BSA, 66.3 kDa), ovalbumin (OA, 46 kDa), carbonic anhydrase (CA, 29 kDa), chymotrypsinogen (Chym, 25 kDa), ribonuclease A (RNA, 13.7 kDa), and cytochrome *c* (Cyt C, 12.5 kDa).

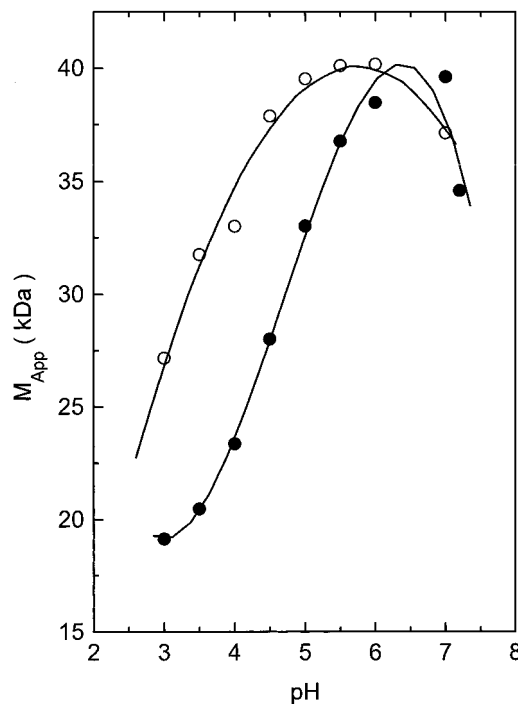


FIGURE 2: pH dependence of the apparent molecular mass of pOBP (●) and BLG (○) based on the gel filtration data.

sponding to the change of the dimer–monomer equilibrium (Figure 2).

To obtain more information about the quaternary structure of pOBP, the ultracentrifugation was carried out with pOBP and BLG in a neutral and acid medium. The results are pre-

Table 1: Sedimentation Coefficients (*S*) of Porcine Odorant Binding Protein (pOBP) and of Bovine β -Lactoglobulin (BLG)

protein	$S \times 10^{13}$ (s)	
	neutral pH	acidic pH
OBP	$1.52^a \pm 0.07$	$1.84^b \pm 0.17$
	$1.54^c \pm 0.07$	—
BLG	$2.73^a \pm 0.05$	$1.51^d \pm 0.08$

^a In 10 mM phosphate and 1 mM EDTA (pH 6.6). ^b In 40 mM glycine (pH 3.5). ^c In 50 mM phosphate and 0.1 M NaCl (pH 7.2). ^d In 40 mM glycine (pH 2.0).

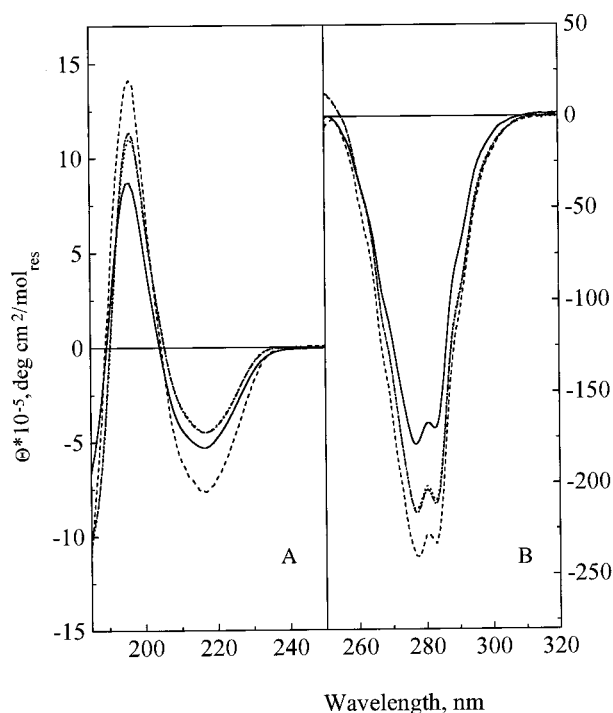


FIGURE 3: CD spectra of pOBP in the far-UV (A) and near-UV (B) regions: (—) pH 6.6 and 25 °C, (---) pH 3.5 and 36 °C, (···) pOBP in the presence of DMO at a ligand:protein ratio of 2:1, at pH 6.6 and 25 °C, and (-·-·-) pOBP in the presence of DMO at a ligand:protein ratio of 4:1, at pH 6.6 and 25 °C.

sented in Table 1. It can be seen that the sedimentation coefficient of pOBP in an acid medium is close to that of BLG. Both of them correspond to the monomeric forms of these lipocalins. The sedimentation coefficient of pOBP does not differ significantly at neutral pH from that observed at acid pH, indicating a monomeric state of the protein. The increase in ionic strength to 0.1 M NaCl does not affect the value of the sedimentation coefficient of pOBP. In contrast, the sedimentation coefficient of BLG at neutral pH corresponds to its dimeric form, as reported in the literature (21–23).

CD spectra of pOBP at pH 6.6 exhibit in the far-UV region a maximum at 196 nm and a minimum at 217 nm (Figure 3A). The deconvolution of the far-UV spectrum of pOBP using Provencher's algorithm (18) revealed about 6% α -helix and 85% β -sheet. A well-pronounced negative band is observed in the aromatic region. Two minima at 277 and 283 nm indicate a highly asymmetric environment of tyrosine residues in the folded structure of pOBP (Figure 3B). No significant perturbations of CD spectra of pOBP in either the far- or near-UV region are found at pH 3.5. Some change in the intensity is observed, but the number and positions of the spectral bands remain unchanged (Figure 3).

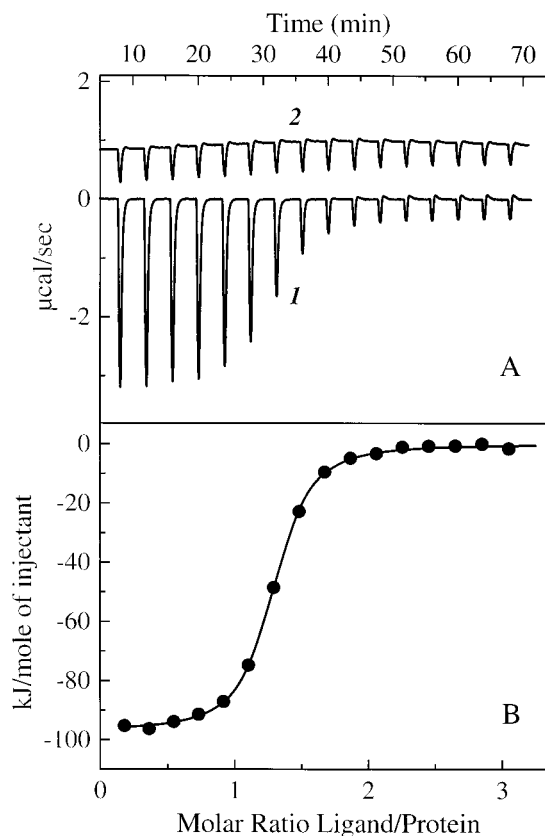


FIGURE 4: Isothermal calorimetric titration curves of pOBP with IBMP. (A) Raw data: curve 1, pOBP in the cell and IBMP in the syringe; and curve 2, buffer in the cell and IBMP in the syringe. (B) The calorimetric binding isotherm for the IBMP–pOBP system: (●) experimental curve and (—) calculated curve obtained as the best fit with an n of 1.220 ± 0.004 , a K_b of $(3.19 \pm 0.16) \times 10^6 \text{ M}^{-1}$, and a ΔH_b of $-97.2 \pm 0.4 \text{ kJ/mol}$. The buffer was 10 mM potassium phosphate and 1 mM EDTA at pH 6.6 and 36 °C.

Isothermal Titration Calorimetry (ITC). Binding tests with purified pOBP were carried out using isothermal titration calorimetry, a direct physical method for assessing ligand–protein interactions. The tested odorants were 2-isobutyl-3-methoxypyrazine (IBMP) and 3,7-dimethyloctan-1-ol (DMO). Titration calorimetric curves obtained for the IBMP–OBP system are presented in Figure 4. The upper panel shows the raw data. Curve 1 is a plot of the heat flow change as a function of time during the injections of a measured volume of ligand solution into the cell containing a protein solution kept at a constant temperature of 36.0 ± 0.5 °C. Curve 2 shows a similar plot for blank titrations, i.e., the injections of the same ligand solution into the buffer without OBP. The heat effect observed during the blank titration is most likely related to the heat of the dilution of ethanol present in ligand solution at about 1%. After integration of each injection peak and correction for the heat of dilution, the values of the enthalpy of mixing for each injection normalized for ligand concentration were plotted as a function of the ligand:protein molar ratio (Figure 4B, ●). The solid line in Figure 4B is a theoretical curve obtained as the best fit of experimental points according to the mathematical model of binding. This model corresponds to the one affinity class of binding. The parameters of fitting were as follows: the association constant, K_b (M^{-1}), the binding enthalpy, ΔH_b (kJ/mol), and the number of binding sites, n , which is a molar binding stoichiometry. The values of

Table 2: Thermodynamic Parameters of Ligand Binding to pOBP at 36 °C According to ITC^a

pH	ligand	<i>n</i>	<i>K_b</i> × 10 ⁻⁶ (M ⁻¹)	Δ <i>H_b</i> (kJ/mol)	<i>T</i> Δ <i>S_b</i> (kJ/mol)	Δ <i>G_b</i> (kJ/mol)
6.6 ^b	IBMP	1.220 ± 0.003	3.19 ± 0.16	-97.2 ± 0.4	-58.7	-38.5
6.6 ^b	DMO	0.800 ± 0.007	4.94 ± 0.43	-87.8 ± 0.7	-48.2	-39.6
4.1 ^c	IBMP	1.080 ± 0.008	2.29 ± 0.28	-64.0 ± 0.7	-26.4	-37.6
3.5 ^d	IBMP	0.417 ± 0.020	0.92 ± 0.23	-67.4 ± 4.4	-32.1	-35.3

^a Calculated per pOBP dimer (35.4 kDa). ^b In 10 mM phosphate and 1 mM EDTA. ^c In 25 mM acetate and 1 mM EDTA. ^d In 40 mM glycine. The values of errors given in columns 2–4 represent the errors of fitting the experimental binding isotherms according to the model with one affinity binding site.

binding parameters derived from the data depicted in Figure 4 are presented in Table 2. At pH 6.6, the binding stoichiometry for the IBMP–OBP interaction is 1.22 per dimer of pOBP which is close to one ligand molecule bound per pOBP homodimer. Calorimetric titration at pH 6.6 was also carried out with DMO as a ligand. Binding parameters for the DMO–OBP system are approximately on the same order of magnitude as those for the IBMP (Table 2).

As it was detected by gel filtration, the homodimer of pOBP dissociates into monomers at an acidic pH (Figure 2). It was important to determine whether a change of the dimer–monomer equilibrium affects the binding capacity of pOBP. Calorimetric binding isotherms obtained for the IBMP–pOBP system at pH 4.1 and 3.5 yielded binding parameters, which are summarized in Table 2. At pH 3.5, pOBP is still able to bind IBMP with high affinity, but the apparent number of binding sites is more than halved.

High-Sensitivity Differential Scanning Calorimetry (HS-DSC). Denaturation thermograms of pOBP alone and pOBP in the presence of IBMP at pH 6.6 are presented in Figure 5. Thermal denaturation of pOBP with and without ligand is essentially reversible at neutral pH and at low ionic strength as detected by reheating of the protein sample in a calorimetric cell (Figure 5, inset). HS-DSC measurements were carried out with pOBP at several pHs below 6.6. Unfortunately, thermal denaturation of pOBP in the vicinity of its isoelectric point (pI 4.1) was accompanied by substantial aggregation of the unfolded protein, which distorted the baseline of the thermogram at temperatures above denaturation temperature (data not shown). For this reason, it was impossible to estimate denaturation enthalpy as a function of pH. The change in stability of pOBP at an acidic pH could be characterized only by the transition temperature. It was observed that the denaturation temperature of pOBP decreases regularly with decreasing pH, approaching room temperature at about pH 1.0. At pH 4.0 and 3.5, the denaturation temperatures of pOBP were 57.7 and 54.4 °C, respectively. These values indicate that pOBP retains its tertiary structure at physiological temperature (36 °C) up till pH 3.5. This conclusion is confirmed by CD spectra of pOBP at pH 3.5 (Figure 3). Thus, the dissociation of the pOBP dimer at an acidic pH does not lead to the denaturation of the pOBP monomer, and the ITC data obtained at pH 4.1 and 3.5 (Table 2) concern the protein still retaining its tertiary structure.

Thermodynamic denaturation parameters of pOBP determined at pH 6.6 are presented in Table 3. Under these conditions, pOBP is characterized by a transition temperature *T_d* of 69.23 ± 0.29 °C and calorimetric enthalpy Δ*H_{cal}* of

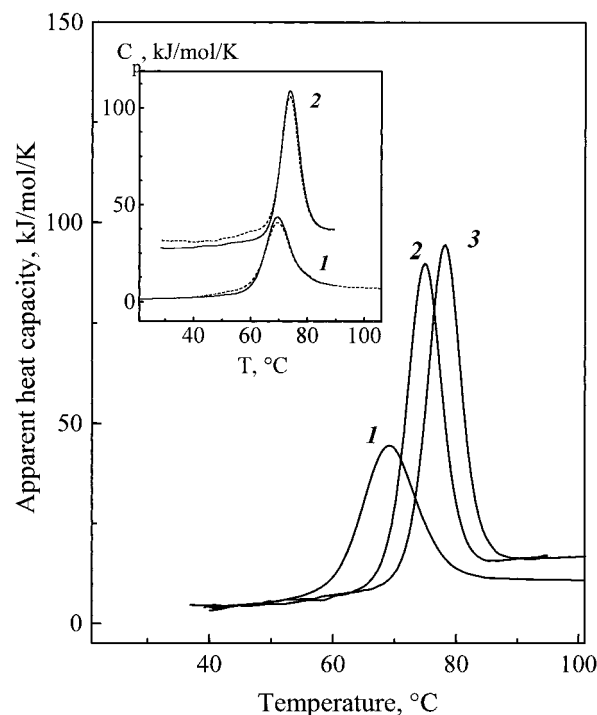


FIGURE 5: Denaturation heat capacity curves of pOBP (1) and pOBP in the presence of IBMP (2) and DMO (3) at pH 6.6. The protein concentration was 0.015–0.020 mM; the ligand:protein molar ratio was 9:1, and the heating rate was 60 K/h. The buffer was 10 mM potassium phosphate and 1 mM EDTA. (Inset) Heat capacity curves of pOBP (1) and pOBP in the presence of IBMP (2) obtained during the first (solid line) and second (dashed line) calorimetric scans. The ligand:protein molar ratio was 2:1.

391.1 ± 17.2 kJ/mol per subunit of OBP. The value of theoretical (van't Hoff) enthalpy (Δ*H_{VH}*) is equal to 392.2 ± 14.5 kJ/mol. This corresponds to a Δ*H_{cal}*/Δ*H_{VH}* ratio of 0.997 ± 0.013 which suggests a two-state mechanism of unfolding on the level of the pOBP monomer. The value of the denaturation heat capacity increment (Δ*C_p* = 3.98 ± 1.39 kJ mol⁻¹ K⁻¹) was determined with low precision because of the instability of the heat capacity baseline in the postdenaturation region of pOBP thermograms.

Denaturation thermograms of pOBP at pH 6.6 in the presence of IBMP and DMO are shown in Figure 5. The transition peak in the presence of ligands is well-reproduced during reheating of the sample in a calorimetric cell (Figure 5, inset). Both ligands markedly affect the unfolding transition of pOBP, shifting it to higher temperatures and increasing the enthalpy compared with that of the unliganded protein. The corresponding thermodynamic parameters are given in Table 3. An increasing transition temperature of a protein in the presence of a ligand is indicative of a specific binding with the protein in its native state (24). It should be noted that the highest total concentrations of IBMP and DMO in the sample were 0.125 and 0.139 mM, respectively. This is too small to exert nonspecific effects on protein denaturation equilibrium. However, this concentration was sufficient to ensure an excess of ligand (about 9-fold) with respect to protein concentration, leading to saturation of binding sites. CD spectra of pOBP are shown in the presence of DMO at ligand:protein ratios of 2:1 and 4:1 (per monomer) (Figure 3). No changes in the spectrum induced by the ligand can be observed. This indicates that ligand binding does not alter the structure of pOBP. Hence, the stabilization of pOBP

Table 3: Thermodynamic Parameters of the Denaturation of pOBP in the Presence of Ligands [10 mM phosphate and 1 mM EDTA (pH 6.6)]

ligand	C_p (mmol of monomer)	C_L (mM)	T_d (°C)	ΔH_{cal} (kJ/mol)	ΔH_{VH} (kJ/mol)	ΔC_p (kJ mol ⁻¹ K ⁻¹)	$\Delta H_{cal}/\Delta H_{VH}$
none	0.023	0	69.15	374.2	369.2	5.30	1.014
	0.029		69.09	379.5	384.6	3.97	0.987
	0.018		68.77	366.6	377.8	2.73	0.971
	0.028		69.53	389.5	393.3	nd ^h	0.990
	0.021		69.45	404.2	401.1	2.33	1.008
	0.019		68.93	390.3	394.6	5.86	0.989
	0.021		69.08	391.3	390.1	3.69	1.003
	0.014		69.81	433.0	427.1	nd	1.014
			69.23 ± 0.29 ^a	391.1 ± 17.2 ^a	392.2 ± 14.5 ^a	3.98 ± 1.39 ^b	0.997 ± 0.013 ^a
IBMP	0.008	0.017	73.72	579.6	544.7	6.82	1.064
IBMP	0.014	0.125	74.85	593.6	593.2	6.62	1.001
DMO	0.015	0.139	77.95	581.6	582.4	6.72	0.999
ALDSon ^c	0.010	0.094	68.58	443.9	429.4	6.25	1.034
ANDSan ^d	0.009	0.091	68.83	392.9	396.1	nd	0.992
ANDSen ^e	0.006	0.066	68.84	393.7	410.2	5.68	0.960
LPDC ^f	0.014	0.126	70.07	484.1	474.6	5.23	1.020
CAP ^g	0.011	0.100	68.88	454.6	454.4	6.93	1.001

^a Estimated at the 95% confidence level. ^b Standard deviation. ^c Aldosterone. ^d 5 α -Androstan-17 β -ol-3-one. ^e 5-Androsten-3 β -ol-17-one (dehydroandrosterone). ^f Lysophosphatidylcholine (C₁₆). ^g Capsaicin. ^h Not determined.

observed in HS-DSC in the presence of ligands can be attributed to a shift of the denaturation equilibrium toward the folded form of the protein but not to the ligand-induced change of the folded structure.

As can be seen in Figure 5, DMO has a more pronounced effect on the transition temperature of pOBP than IBMP at the same ligand:protein ratio. It was shown that the increment of transition temperature of a protein in the presence of ligand is related to the value of the association constant, K_b (24). It may be concluded that at high temperatures DMO binds to pOBP with a higher constant than IBMP. This result corresponds to the higher value of K_b for DMO detected by ITC at low temperatures (Table 2).

Thus, HS-DSC data can serve to test the interactions of pOBP with its ligands. The advantage of this technique is the substantially lower (about 10-fold) amount of the protein needed as compared to that with ITC. Table 3 summarizes calorimetric transition parameters of pOBP in the presence of different potential ligands: steroid hormones, phospholipids (LPDC), and capsaicin. One can see that most of these substances, except LPDC, affect neither the transition temperature nor the unfolding mechanism of pOBP. A slight increase in the transition temperature and enthalpy was detected for LPDC, implying the existence of a weak interaction with pOBP.

DISCUSSION

The molecular mass of purified pOBP (17.7 kDa) determined by mass spectrometry as well as its isoelectric point (pI 4.1) estimated by IEF coincides with the corresponding theoretical values (17.707 kDa and pI 4.18) predicted from the pOBP sequence (Swiss-Prot entry P81245). These features and the existence of binding affinity for IBMP confirm the identity of the purified protein as that of porcine OBP. According to SDS-PAGE, pOBP migrates in the gel with an apparent molecular mass of 22 kDa. The same value for pOBP was obtained by SDS-PAGE previously (7). The difference in the molecular mass of pOBP estimated by SDS-PAGE and mass spectrometry seems to be too large to be explained by the presence of an endogenous ligand dissociating during ionization applied in mass spectrometry. Admittedly, the deviation of the molecular mass of pOBP

estimated by SDS-PAGE from that measured by mass spectrometry indicates an unusual binding of SDS with pOBP. It was found previously in the case of several proteins that abnormal binding of SDS can result from the peculiar sequence of a protein (25–27).

Gel filtration chromatography shows a dimeric form of pOBP at pH 6–7 and a monomeric form at pH 3–4. A single elution peak is observed between pH 7.0 and 3.0, indicating no separation of dimers and monomers under elution conditions. However, a continuous decrease in the apparent molecular mass of pOBP can be detected when changing the pH from 7.0 to 3.0 (Figure 2). The same tendency can be observed in a case of bovine β -lactoglobulin (BLG) under the same experimental conditions (Figure 2). It is well-known that BLG is a 38 kDa homodimer at neutral pH and dissociates to monomers in an acidic medium at low ionic strength (22, 23). A detection by gel filtration of the continuous decrease in the apparent molecular mass of BLG with decreasing pH can be attributed to its dissociation. This fact proves the pertinence of the applied gel filtration conditions for characterization of the dimer–monomer equilibrium in pOBP and its dependence on pH. The failure to resolve BLG and pOBP dimers and monomers by gel filtration can be explained by the existence of a fast equilibrium between these two protein isoforms. In the case of systems with fast association/re-equilibration, no resolution of monomers and dimers can be predicted by theoretic analysis of mass transport processes such as gel filtration, ultracentrifugation, and gel electrophoresis (28, 29). In this case, the elution volume of the sample will be a function of the average apparent association constant under given conditions. Thus, the results of gel filtration suggest that pOBP exists preferentially in a dimeric form at pH 6–7 and in a monomeric form at pH 3–4. It should be concluded from Figure 2 that the dimer of pOBP is substantially less stable than that of BLG.

The instability of the pOBP quaternary structure is indirectly confirmed by the data from ultracentrifugation. This method detects the existence of the monomeric form of this protein at neutral pH under experimental conditions identical with those applied during gel filtration (Table 1). It is believed that ultracentrifugation presents an advantage

in characterization of quaternary structure of proteins as compared with gel filtration. It should, however, be highlighted that high pressures are usually generated at high speeds in the sedimentation cell (about several hundred atmospheres) (21). In the case of monomeric proteins, the dependence of the sedimentation coefficient on pressure is negligible. However, in the case of oligomeric proteins, the association constant decreases markedly under pressure (30). The effect of pressure can lead to changes in the quaternary structure of oligomeric proteins similar to changes observed at moderate concentrations of denaturants. Several examples of protein subunit dissociation induced by pressure in the range of 0.3–3 kbar were reported in the literature (31–34). The effect of pressure on the dimerization constant of pOBP could be an interesting subject of a separate study.

Thus, at physiologic pH, pOBP is dimeric which reminds us of what was already observed in the case of bovine and rabbit OBPs (7). Existence of pOBP dimers was detected in all protein preparations independent of the origin of the raw material, pig race, or sex. This result differs from previous reports of a uniquely monomeric form of pOBP (7, 14). With respect to the proposed instability of the pOBP dimer, it is plausible that this divergence of results on the quaternary structure of pOBP takes root in differences in applied experimental conditions. The interesting dimerization mechanism of bovine OBP proceeding by domain swapping reported by Brownlow and Sawyer (13) and by Tegoni et al. (11) does not exist in porcine OBP as demonstrated by crystallography (14). Thus, dimerization of porcine OBP should be somewhat different from that of its bovine counterpart.

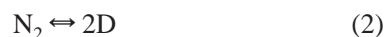
As shown by HS-DSC (Figure 5, inset), thermal unfolding of pOBP is reversible at physiological pH. This allows the application of the equilibrium thermodynamic approach for the analysis of the unfolding transition of pOBP. A typical DSC scan for pOBP normalized per monomer in the absence of ligand is presented in Figure 6. The analysis of the transition profile was carried out using two models. The first model is a simple two-state transition:



or



This assumes that denaturation is not accompanied by dimer dissociation and also means that the dissociation either precedes the denaturation (eq 1) or does not occur at all; i.e., denatured pOBP exists in a dimeric form (eq 1a). The second model used for analysis is a two-state transition conjugated with dissociation:



This model assumes that the protein remains dimeric up to the denaturation temperature and then undergoes simultaneous denaturation and dissociation (35, 36). Transition curves obtained as the best fit of experimental points according to two models are shown in Figure 6. The inset of Figure 6 shows the deviations of the calculated heat capacities at each temperature from the experimental values obtained by two models. It is seen that eqs 1 and 1a show a statistical distribution of deviations, while eq 2 gives

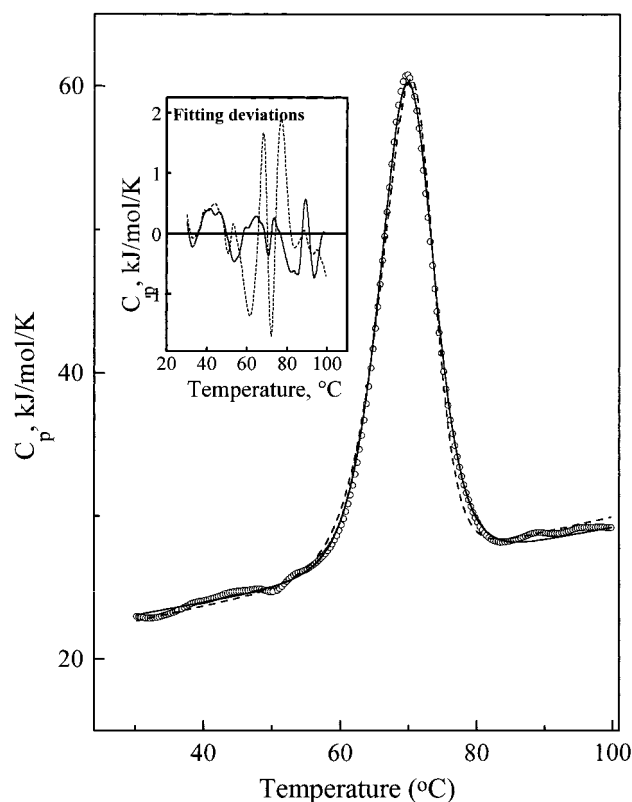


FIGURE 6: Denaturation heat capacity curve of pOBP at pH 6.6: (○) experimental curve, (—) two-state fitting according to the model without dissociation (see eqs 1 and 1a in the text), and (---) two-state fitting according to the model with dissociation (see eq 2 in the text). (Inset) The deviation from experimental points of the fitting according to eqs 1 and 1a (—) and to eq 2 (---).

systematic deviations in the area of the transition peak. The values of the standard deviation σ of the fitting by eqs 1 and 1a, and eq 2, are equal to 0.31, and 0.73, respectively. Thus, eqs 1 and 1a approximate better the experimental data. It means that the thermal denaturation of pOBP is not related to the dissociation of its dimer.

It is also unlikely that the pOBP dimer is stable at temperatures above the denaturation temperature. The CD spectrum of thermally denatured pOBP (at 85 °C) is broadly similar to the CD spectrum of completely unfolded pOBP in 8 M urea (Figure 7). Such a highly disordered structure would hardly be able to retain native-like contacts between monomers. Consequently, dissociation of pOBP dimers should occur most likely at temperatures below denaturation temperature. This confirms obviously extremely weak interactions between monomers of pOBP suggested from the data of gel filtration and velocity sedimentation. HS-DSC does not detect any heat effect which could be attributed to the dimer dissociation at temperatures below that of denaturation. This implies that porcine OBP dimer dissociates in a noncooperative manner, i.e., with low enthalpy.

The direct assessment of ligand–pOBP interactions carried out by ITC yields the values of binding parameters (K_b and ΔH_b) and stoichiometry (n). These values can serve in calculating the Gibbs free energy, ΔG_b , and the entropy, ΔS_b , of binding according to the following equations:

$$\Delta G_b = -RT \ln K_b \quad (3)$$

$$T\Delta S_b = \Delta H_b - \Delta G_b \quad (4)$$

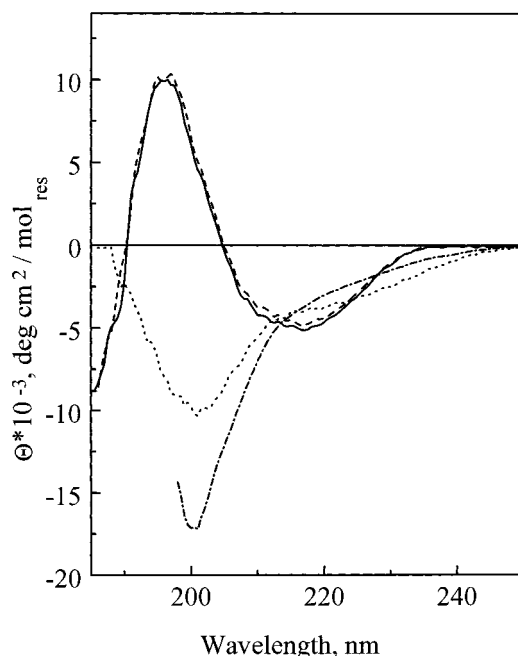


FIGURE 7: CD spectra of pOBP in the far-UV spectral region: (—) native pOBP at 25 °C, (···) pOBP at 85 °C, (---) pOBP heated to 85 °C and cooled to 25 °C, and (-·-·-) pOBP in 8 M urea. The buffer was 10 mM potassium phosphate and 1 mM EDTA (pH 6.6).

All these thermodynamic parameters for IBMP–pOBP and DMO–pOBP systems are summarized in Table 2.

The model of one affinity binding site gives the best fit for calorimetric binding isotherms obtained with both IBMP and DMO as ligands. At neutral pH, the binding stoichiometry for these ligands is close to one molecule of ligand per pOBP dimer. The interaction of pOBP with IBMP and DMO is accompanied by a favorable (negative) net change in enthalpy which is relatively elevated when compared with those observed in the majority of ligand–protein systems studied until now (37). In contrast, the net change of entropy under binding conditions is unfavorable (negative). This enthalpy–entropy balance results in moderate values of free energy of binding for both ligands (Table 2).

A decrease in binding enthalpy is observed for the IBMP–pOBP system at an acidic pH. This could not be related to the protonation of protein groups caused by ligand binding because the enthalpy values determined in acetate and glycine buffers are on the same order of magnitude within the accuracy of the experiment (Table 2). Decreasing binding enthalpy is accompanied by a decrease in the unfavorable change of entropy so that the Gibbs energy does not vary substantially. Thus, pOBP at an acidic pH reveals apparently the same affinity for IBMP as at physiological pH, suggesting that the binding mechanism remains uniform despite this rather harsh pH variation.

At an acidic pH, a substantial decrease in parameter n is observed in the case of IBMP (Table 2). This is not, however, a consequence of partial acid denaturation of the protein as could be thought. As was verified by HS-DSC, the denaturation temperature of pOBP at pH 3.5 is 54.4 °C which is well above the temperature of ITC measurements (36.0 °C). When the fact that at pH 3.5 unliganded pOBP is monomeric is taken into account, it is evident that the binding of ligand

under these conditions is accompanied by a shift of the dimer–monomer equilibrium:



where N, N_2 , and L represent protein monomer, protein dimer, and ligand, respectively. This means that binding of the ligand induces porcine OBP dimerization even under conditions in which its apo form is completely dissociated.

The shift of the transition temperature of pOBP induced by IBMP and DMO (Figure 5) suggests that these ligands are bound to the protein with a substantial association constant even at the denaturation temperature and that they dissociate simultaneously with pOBP unfolding (24, 38). Hence, strongly bound ligands might stabilize the dimeric form of pOBP not only at low pH but also at high temperatures up to the unfolding temperature. This possibility can be verified by a detailed thermodynamic analysis of the unfolding profile of pOBP obtained at different ligand concentrations. Additionally, the elucidation of the transition mechanism of pOBP in the presence of ligands would allow the precise calculation of the binding parameters, association constant, and binding enthalpy, at high temperatures (24).

The net change in enthalpy and entropy under ligand binding conditions is a sum of contributions of different interactions: polar interactions (hydrogen bonding and ion pairs), nonpolar interactions (van der Waals contacts, including aliphatic and aromatic groups), and hydration effects. Hydration effects at physiological temperatures are considered entropically favorable (39) and, thus, could not be the driving force in pOBP binding. Hydrogen bonding and van der Waals interactions are enthalpically driven (39). As was indicated by CD measurements of porcine OBP spectra in the near-UV region, the state of its aromatic residues does not show significant changes in the presence of ligand (DMO) (Figure 3B). For this reason, the contribution of aromatic residues of pOBP to the interaction with ligand can be neglected. A remarkably high negative binding enthalpy of pOBP implies a dominating contribution of aliphatic van der Waals contacts and/or of polar interactions (hydrogen bonding) in ligand binding to pOBP (37, 39).

An enthalpically driven interaction of pOBP with IBMP and DMO is confirmed by the analysis of HS-DSC data. For example, at saturating IBMP concentrations, the value of the calorimetric enthalpy is by 405 kJ/mol per dimer higher than in the absence of ligand (Table 3). After correction of this value for the enthalpy increase related to the temperature dependence of unfolding enthalpy assuming a $T_{d,0}$ of 69.23 °C, a $T_{d,L}$ of 74.85 °C, and a ΔC_p of 13.24 kJ/mol of dimer (Table 3), we obtain the value of 330.6 kJ/mol of dimer. This is the enthalpy of ligand dissociation, ΔH_{dis} , accompanying protein unfolding. When the fact that $\Delta H_{dis} = -\Delta H_b$ is taken into account, the binding enthalpy $\Delta H_b(74.85 \text{ °C})$ can be determined (–330.6 kJ/mol of dimer). Consequently, the enthalpy of binding at high temperatures is more negative than at physiological temperatures [$\Delta H_b(36 \text{ °C}) = -97.2 \text{ kJ/mol}$]. This tendency is consistent with a negative heat capacity increment of binding, $\Delta C_{p,b}$, observed for IBMP. Crude estimation of $\Delta C_{p,b}$ using binding enthalpy values for $\Delta H_b(36.0 \text{ °C})$ of –97.2 kJ/mol and for

ΔH_b (74.85 °C) of -330.6 kJ/mol yields for the binding heat capacity increment $\Delta C_{p,b}$ a value of -6.0 kJ/mol for the dimer which is -3.0 kJ/mol for the pOBP monomer. It should be highlighted that the value of $\Delta C_{p,b}$ computed from the difference between directly measured HS-DSC heat capacity increments of liganded and nonliganded pOBP equals -2.64 kJ/mol. This is close to the $\Delta C_{p,b}$ value of -3.0 kJ/mol estimated above from the enthalpy changes and thus confirms the suggested change of binding enthalpy at high temperatures. The same pattern can be seen in the case of binding of DMO by pOBP (Table 3). Negative values of binding heat capacity increment are a widely discussed feature of ligand-protein interactions (37).

The value of the binding heat capacity increment is a very sensitive parameter that indicates a change in the hydration state of the protein binding sites and of ligand. A negative value of this parameter results from the screening of apolar groups from an aqueous phase. Usually, such a dehydration of apolar groups leads to a positive change in the entropy. The net change in entropy observed in the case of pOBP-IBMP and pOBP-DMO interactions happens to be negative (Table 2), indicating that a positive entropy contribution from dehydration of apolar groups is insignificant.

Studied nonvolatile ligands show little tendency to interact specifically with pOBP. As detected by HS-DSC, steroid hormones do not affect the transition temperature, or the enthalpy (Table 3). pOBP can hardly be considered as a protein playing an important role in sexual communication in contrast to odor binding lipocalins recently purified from boar salivary glands (40). Capsaicin does not affect the transition temperature of pOBP. However, it increases somewhat the transition enthalpy and the heat capacity increment of pOBP (Table 3). The similar effect characterized by an additional increase in the transition temperature of pOBP is produced by phospholipids (Table 3). These facts demonstrate the existence of weak (nonspecific) interactions of these substances with pOBP, which may be binding to different categories of binding sites.

ACKNOWLEDGMENT

We thank Mr. A. L. Leontiev for his technical assistance in velocity sedimentation and Prof. V. Ya. Grinberg for his useful discussions.

REFERENCES

1. Flower, D. R. (1996) *Biochem. J.* 318, 1–14.
2. Pelosi, P., Baldaccini, N. E., and Pisanelli, A. M. (1982) *Biochem. J.* 201, 245–248.
3. Bignetti, E., Cavaggioni, A., Pelosi, P., Persaud, K. C., Sorbi, R. T., and Tirindelli, R. (1985) *Eur. J. Biochem.* 149, 227–231.
4. Pevsner, J., Trifiletti, R. R., Strittmatter, S. M., and Snyder, S. H. (1985) *Proc. Natl. Acad. Sci. U.S.A.* 82, 3050–3054.
5. Pevsner, J., Hwang, P. M., Sklar, P. B., Venable, J. C., and Snyder, S. H. (1988) *Proc. Natl. Acad. Sci. U.S.A.* 8, 2383–2387.
6. Pes, D., Dal Monte, M., Ganni, M., and Pelosi, P. (1992) *Comp. Biochem. Physiol.* 103B, 1011–1017.
7. Dal Monte, M., Andreini, I., Revoltella, R., and Pelosi, P. (1991) *Comp. Biochem. Physiol.* 99B, 445–451.
8. Baldaccini, N. E., Gagliardo, A., Pelosi, P., and Topazzini, A. (1986) *Comp. Biochem. Physiol.* 84B, 249–253.
9. Pevsner, J., Hou, V., Snowman, A. M., and Snyder, S. H. (1990) *J. Biol. Chem.* 265, 6118–6125.
10. Bignetti, E., Cattaneo, P., Cavaggioni, A., Damiani, G., and Tirindelli, R. (1988) *Comp. Biochem. Physiol.* 90B, 1–5.
11. Tegoni, M., Ramoni, R., Bignetti, E., Spinelli, S., and Cambillau, C. (1996) *Nat. Struct. Biol.* 3, 902–906.
12. Bianchet, M. A., Bains, G., Pelosi, P., Pevsner, J., Snyder, S. H., Monaco, H. L., and Amzel, L. M. (1996) *Nat. Struct. Biol.* 3, 934–939.
13. Brownlow, S., and Sawyer, L. (1996) *Nat. Struct. Biol.* 3, 902–906.
14. Spinelli, S., Ramoni, R., Grolli, S., Bonicel, J., Cambillau, C., and Tegoni, M. (1998) *Biochemistry* 37, 7913–7918.
15. Bychkova, V. E., Berni, R., Rossi, G. L., Kutysenko, V. P., and Ptitsyn, O. B. (1992) *Biochemistry* 31, 7566–7571.
16. Folch, J., Lees, M., and Sloane-Stanley, G. H. (1957) *J. Biol. Chem.* 226, 497–509.
17. Smith, R. D., Loo, J. A., Edmonds, C. G., Barinaga, C. J., and Udseth, H. R. (1990) *Anal. Chem.* 62, 882–899.
18. Provencher, S. W., and Glöckner, J. (1981) *Biochemistry* 20, 33–37.
19. Pace, C. N., Vajdos, F., Fee, L., Grimsley, G., and Gray, T. (1995) *Protein Sci.* 4, 2411–2423.
20. Paolini, S., Tanfani, F., Fini, C., Bertoli, E., and Pelosi, P. (1999) *Biochim. Biophys. Acta* 1431, 179–188.
21. Tanford, C. (1961) in *Physical Chemistry of Macromolecules*, Chapter 6, pp 317–456, John Wiley & Sons, New York.
22. Hambling, S. G., McAlpine, A. S., and Sawyer, L. (1992) in *Advanced Dairy Chemistry-1: Proteins* (Fox, P. F., Ed.) pp 141–190, Elsevier Applied Science, New York.
23. Aymard, P., Durand, D., and Nicolai, T. (1996) *Int. J. Biol. Macromol.* 19, 213–221.
24. Brands, J. F., and Lin, L.-N. (1990) *Biochemistry* 29, 6927–6940.
25. Weber, K., Pringle, J. R., and Osborn, M. (1972) *Methods Enzymol.* 26, 3–27.
26. Nielsen, T. B., and Reynolds, A. (1978) *Methods Enzymol.* 48, 3–10.
27. Noel, D., Nikaido, K., and Ames, G. F.-L. (1979) *Biochemistry* 18, 4159–4166.
28. Cann, J. R., and Kegeles, G. (1974) *Biochemistry* 13, 1868–1874.
29. Kegeles, G., and Cann, J. R. (1978) *Methods Enzymol.* 48, 248–270.
30. Harrington, W. F., and Kegeles, G. (1973) *Methods Enzymol.* 27, 306–346.
31. Plager, D. A., and Nelsestuen, G. L. (1992) *Protein Sci.* 1, 530–539.
32. Gross, M., and Jaenicke, R. (1994) *Eur. J. Biochem.* 221, 617–630.
33. Cioni, P., and Strambini, G. B. (1996) *J. Mol. Biol.* 263, 789–799.
34. Bonafe, C. F., Araujo, J. R., and Silva, J. L. (1994) *Biochemistry* 33, 2651–2660.
35. Takahashi, K., and Sturtevant, J. M. (1981) *Biochemistry* 20, 6185–6190.
36. Manly, S. P., Matthews, K. S., and Sturtevant, J. M. (1985) *Biochemistry* 24, 3842–3846.
37. Fisher, H. F., and Singh, N. (1995) *Methods Enzymol.* 259, 194–221.
38. Fukada, H., Sturtevant, J. M., and Quiocho, F. (1983) *J. Biol. Chem.* 258, 13193–13198.
39. Makhatadze, G. I., and Privalov, P. L. (1995) *Adv. Protein Chem.* 47, 307–425.
40. Marchese, S., Pes, D., Scaloni, A., Carbone, V., and Pelosi, P. (1998) *Eur. J. Biochem.* 252, 563–568.

BI990769S